EXPERIMENTAL EVALUATION OF CONFINEMENT REINFORCEMENT IN PRETENSIONED I-GIRDERS

Brandon E. Ross, PE, University of Florida, Gainesville, FL
Gary R. Consolazio, PhD, University of Florida, Gainesville, FL
H.R. (Trey) Hamilton, PhD, PE, University of Florida, Gainesville, FL

ABSTRACT

Precast, pretensioned bridge girders are typically required to have confinement reinforcement placed around the prestressing strands at the end of the member. Crack control during prestress transfer and ultimate strength are generally thought to be improved by the addition of such reinforcement. The role of confinement, however, is not well-understood and is currently detailed using empirical code provisions. This paper will present the results of experimental tests on full scale bridge girders that were conducted to better understand the role and effect of confinement reinforcement. Four tests were conducted on 54in.-deep Florida I-beams (FIB). Specimens were loaded in 3-point bending at a shear span-to-depth ratio near 1.8. Confinement reinforcement was installed in the specimens for two of the tests and was excluded in the other two. Strains in the confinement reinforcement and embedded steel bearing plates were monitored during load testing. Specimens with confinement reinforcement failed in a web-shear failure mode. Those without confinement failed in a lateral-splitting mode, wherein the outside edges of the bottom flange peeled away during testing and the cross-section split apart laterally at ultimate load. Detailed results and findings will be presented and conclusions drawn regarding the effectiveness of confinement reinforcement.

Keywords: Confinement Reinforcement, Pretensioned Girders, Bearing Plates, Flange Splitting, End Region

INTRODUCTION

Confinement reinforcement is placed around prestressing strands in the bottom bulb at the end of pretensioned concrete girders. It serves three primary functions. First, it controls cracking in the bottom flange during prestress transfer and under service loads[1]. Second, it mitigates lateral-splitting failure of the bottom flange at ultimate load[2-4]. Third, it assists in maintaining partial bond capacity between prestressing strands and concrete after cracks form within the transfer length[4-5]. Confinement reinforcement performs these functions by resisting transverse tensile stresses—caused by prestressing and reaction forces—in the bottom flange near the end of the girder.

By performing these functions, confinement reinforcement improves both shear capacity [2,4,6] and ductility[4-5]. It has also been reported that confinement reinforcement does not prevent[4-5] or delay[4] strand slip, and that it has negligible effect on transfer length[1,5,7]. The effects of confinement reinforcement on strand development length are yet to be determined[5].

The 2007 AASHTO LRFD Bridge Design Specifications[8] require that confinement reinforcement be placed around prestressing strands in the bottom bulb of pretensioned concrete beams. Section 5.10.10.2 states: "For the distance 1.5d from the end of the beams … reinforcement shall be placed to confine the prestressing steel in the bottom flange. The reinforcement shall not be less than No. 3 deformed bars, with spacing not exceeding 6.0in. [152mm] and shaped to enclose the strands." These prescriptive requirements do not explicitly address the functions of confinement reinforcement, and are based on limited experimental data.

In this study, an experimental program was conducted to expand the available data regarding confinement reinforcement. The test program focused on determining stress in confinement reinforcement at ultimate load; distance from end where confinement is most effective; and effectiveness of embedded steel bearing plates in providing bottom flange confinement. Results from the research program will be useful for evaluating the current AASHTO requirements and for future development of a confinement reinforcement design procedure.

Many states, including Florida, Washington, and Nebraska have initiated use of I-girder cross-sections with relatively wide, slender bottom flanges. Bottom flange size and shape in these sections does not vary with girder depth. Experimental results from the current research program will be useful for evaluating the implications of slender bottom flanges on girder capacity and behavior. Load tests on Nebraska[5] and Washington[11] girders with wide bottom flanges have previously been reported, however the current program is the first to use the Florida I-Beams (FIB).

EXPERIMENTAL PROGRAM SETUP AND DETAILS

Full-scale load tests were conducted using two 54in. deep Florida I-beams (FIB-54). Test girders were 49ft-6in. long. Each end of each girder was tested, resulting in four separate tests. Each end had a unique combination of variables and will be referred to in this paper as a separate specimen. Variables in the test program included the presence or absence of confinement reinforcement and the quantity of horizontal and vertical reinforcement in the end region. Specimen labels and variables are shown in Fig. 1.
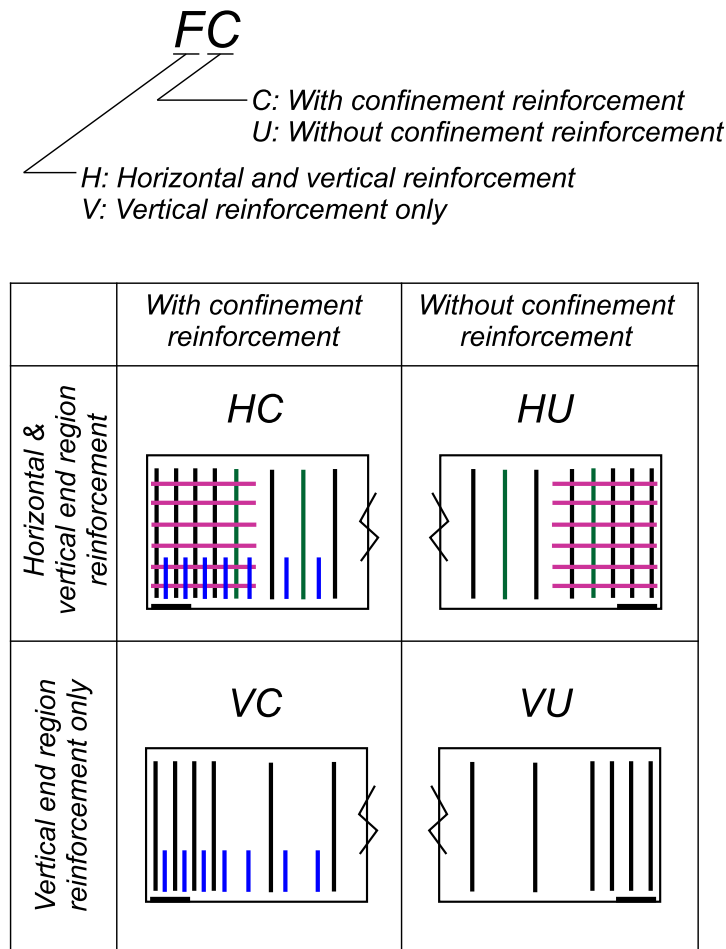

Fig. 1 Specimen Labels and Variables

Specimen detailing (Fig. 2) was based on FDOT design standards[9]. These standards specify that horizontal bars extend beyond the girder end and hook into cast-in-place end diaphragms for development. As the test girders did not have end diaphragms, headed anchors were used to develop horizontal reinforcement in specimens HC and HU. Confinement reinforcement in specimens HC and VC had tighter spacing, but extended over a shorter length from the end than required by AASHTO LRFD. A comprehensive presentation of specimen details will be available in a forthcoming report for the FDOT[10].

Specimens were fabricated in Leesburg, FL by Dura-Stress Inc. After fabrication test girders were trucked to the FDOT M.H. Ansley Structures Research Center in Tallahassee, FL, where cast-in-place decks were poured and the specimens were tested. Specimens had no skew and were tested without end diaphragms. Load, displacement, strand slip, and strain data were continuously collected during testing.

Steel and concrete samples were tested to determine the as-built material properties of the specimens. Table 1 lists the specified and tested properties. Properties shown in Fig. 2 are the specified properties.

Specimens were tested in three-point bending as shown in Fig. 3. Load was applied using side-by-side hydraulic actuators at a rate of approximately 0.4 kip/sec. Load was spread from the jacks to the girders through steel plates and a reinforced neoprene bearing pad. Bearing pads were also placed below each support. A reaction frame was used to transmit load from the actuators to the strong floor (Fig. 4).

Each specimen was loaded at least twice. The first loading simulated a service load of approximately 300kip. This load level was selected based on the service shear load of an existing bridge in Clay County, Florida that utilized FIB-54 girders. Once the service load was reached, the load was held constant and cracks were identified and marked. After cracks were marked the load was removed. The final loading determined the specimen's ultimate strength. Load-displacement was plotted and monitored in real-time during the ultimate load test. Load was applied until it was apparent from the load-displacement plot that a peak load had been reached. Cracking was documented after the ultimate load test was complete.

After the first end (specimen) of each girder was tested, the load point and supports were moved and the opposite end was tested. A 9ft-4.5in. shear span was used for each test. With the exception of specimen HU, overall span length was 42ft-10.5in. Span lengths used for specimen HU are shown in Fig. 3.
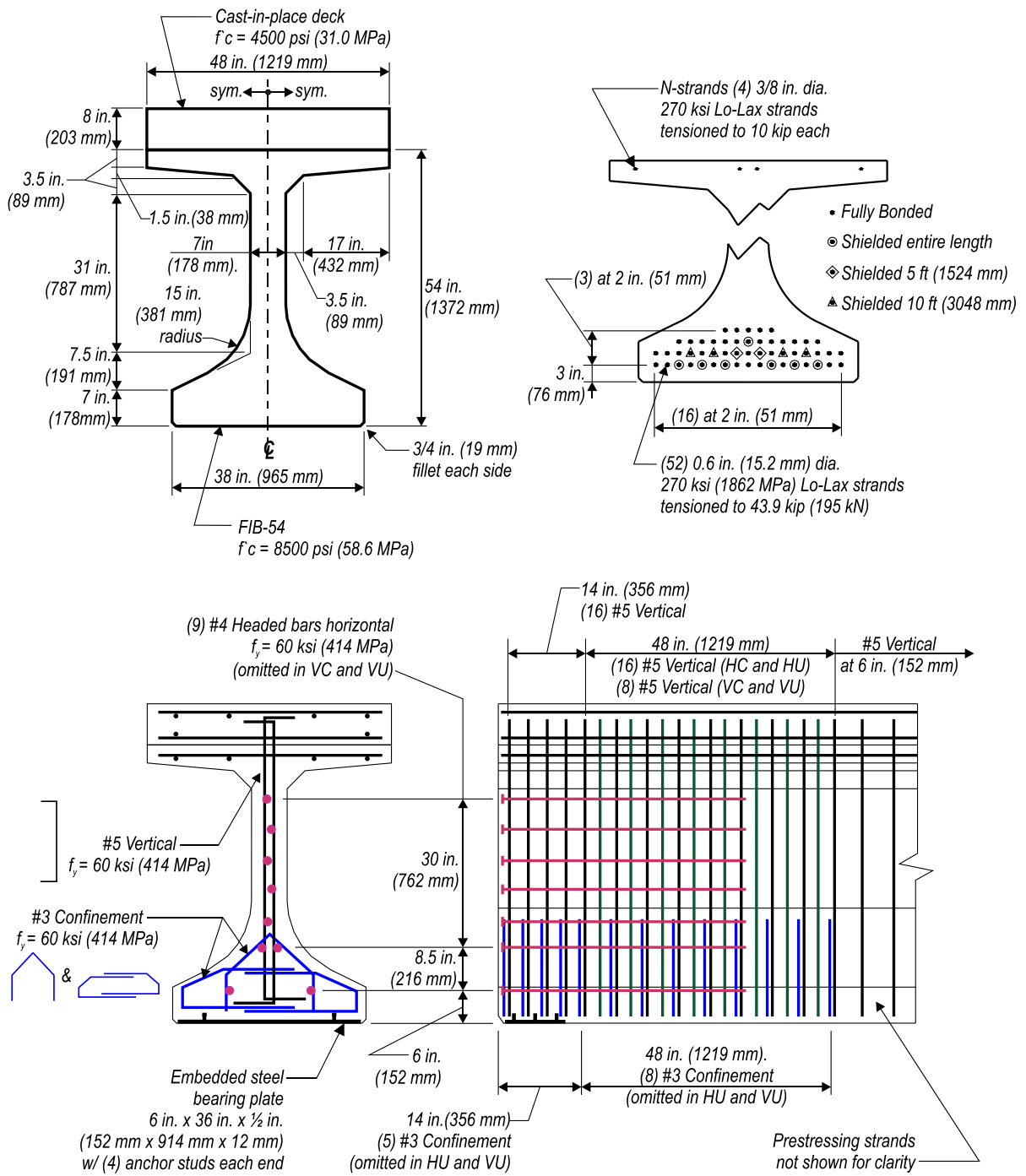
Cast-in-place deck
f'c = 4500 psi (31.0 MPa)
48 in. (1219 mm)
sym. ← → sym.

8 in.
(203 mm)

3.5 in.
(89 mm)

1.5 in.(38 mm)

7in
(178 mm).

17 in.
(432 mm)

31 in.
(787 mm)

15 in.
(381 mm)
radius

3.5 in.
(89 mm)

54 in.
(1372 mm)

7.5 in.
(191 mm)

7 in.
(178mm)

₵

3/4 in. (19 mm)
fillet each side

38 in. (965 mm)

FIB-54
f'c = 8500 psi (58.6 MPa)

N-strands (4) 3/8 in. dia.
270 ksi Lo-Lax strands
tensioned to 10 kip each

(3) at 2 in. (51 mm)

• Fully Bonded
◉ Shielded entire length
◈ Shielded 5 ft (1524 mm)
▲ Shielded 10 ft (3048 mm)

3 in.
(76 mm)

(16) at 2 in. (51 mm)

(52) 0.6 in. (15.2 mm) dia.
270 ksi (1862 MPa) Lo-Lax strands
tensioned to 43.9 kip (195 kN)

14 in. (356 mm)
(16) #5 Vertical

(9) #4 Headed bars horizontal
f_y = 60 ksi (414 MPa)
(omitted in VC and VU)

48 in. (1219 mm)
(16) #5 Vertical (HC and HU)
(8) #5 Vertical (VC and VU)

#5 Vertical
at 6 in. (152 mm)

#5 Vertical
f_y = 60 ksi (414 MPa)

30 in.
(762 mm)

#3 Confinement
f_y = 60 ksi (414 MPa)

&

8.5 in.
(216 mm)

Embedded steel
bearing plate
6 in. x 36 in. x ½ in.
(152 mm x 914 mm x 12 mm)
w/ (4) anchor studs each end

6 in.
(152 mm)

14 in.(356 mm)
(5) #3 Confinement
(omitted in HU and VU)

48 in. (1219 mm).
(8) #3 Confinement
(omitted in HU and VU)

Prestressing strands
not shown for clarity

Fig. 2 Specimen Details

Table 1 Material Properties

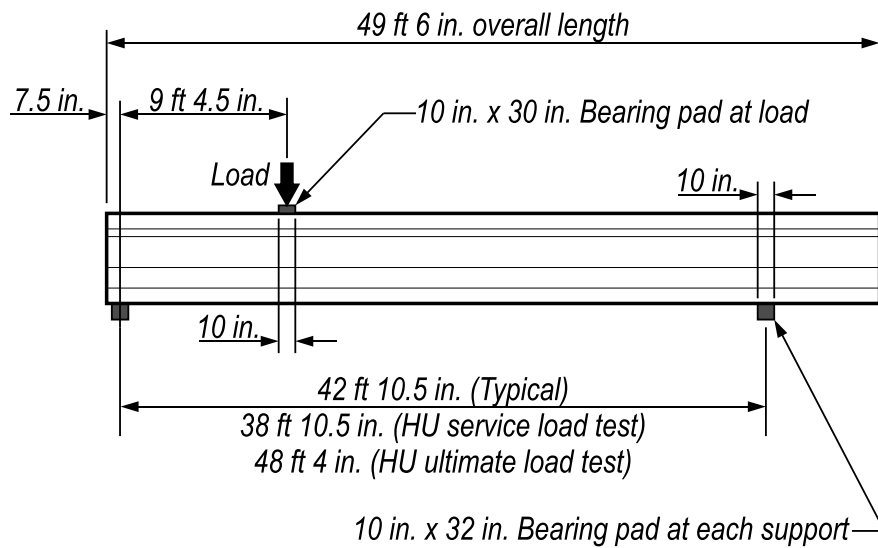| Item	Specified	Tested (average)
Concrete girder	8500 psi (28 day)	8740 psi (28 day)
		10950 psi (test day)
Concrete deck	4500 psi (28 day)	6620 psi (28 day)
		6950 psi (test day)
Mild reinforcement	60 ksi (yield)	68.6 ksi (yield)
Prestressing strand	270 ksi (ultimate)	284 ksi (ultimate)

Fig. 3 Test Setup

Fig. 4 Test Specimen in Load Frame

RESULTS AND DISCUSSION

Load test results are presented in terms of superimposed shear rather than applied load and for the remainder of this paper will be referred to as shear. Superimposed shear is defined as the shear force due to the applied load acting at the support nearest the load point. Self-weight is not included in the superimposed shear.

Displacement results are presented as the vertical displacement occurring at the load point. Displacement at the load point was calculated as the average of the displacements reported by linear variable differential transformers (LVDTs) that were placed on either side of the load. The effects of bearing pad displacement have been removed.

FAILURE MODES

Crushing of the web within the shear span controlled the capacity of specimens with confinement reinforcement (HC and VC). Shortly after web crushing initiated, the top of the specimen displaced longitudinally relative to the lower portion, which signaled that the specimen capacity had been reached. This failure mode is described as web-shear and is the desirable failure mode for this load configuration and arrangement of reinforcement.

Specimens without confinement reinforcement (HU and VU) failed in a lateral-splitting mode, characterized by longitudinal cracks in the bottom flange and by eventual peeling (outward) movement at the edges of the bottom flange (Fig. 5.) Peeling of the bottom flange is caused by eccentricity between prestressing forces in the outer flange and the equal and opposite resultant force centered in the web (Fig. 6.) In the specimens with confinement

reinforcement, peeling movement and longitudinal cracks were restrained, and lateral-splitting failure was mitigated, which resulted in the full effective shear capacity being reached.
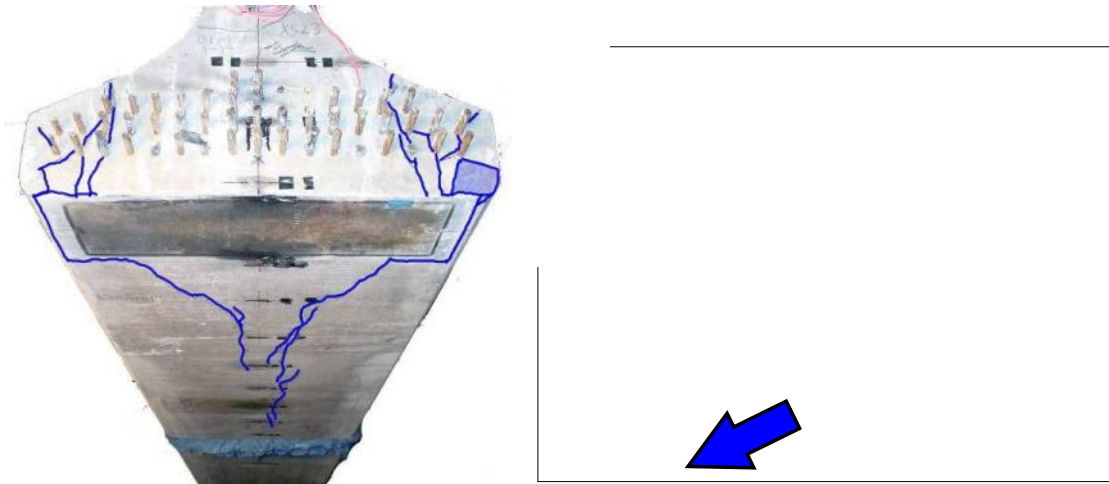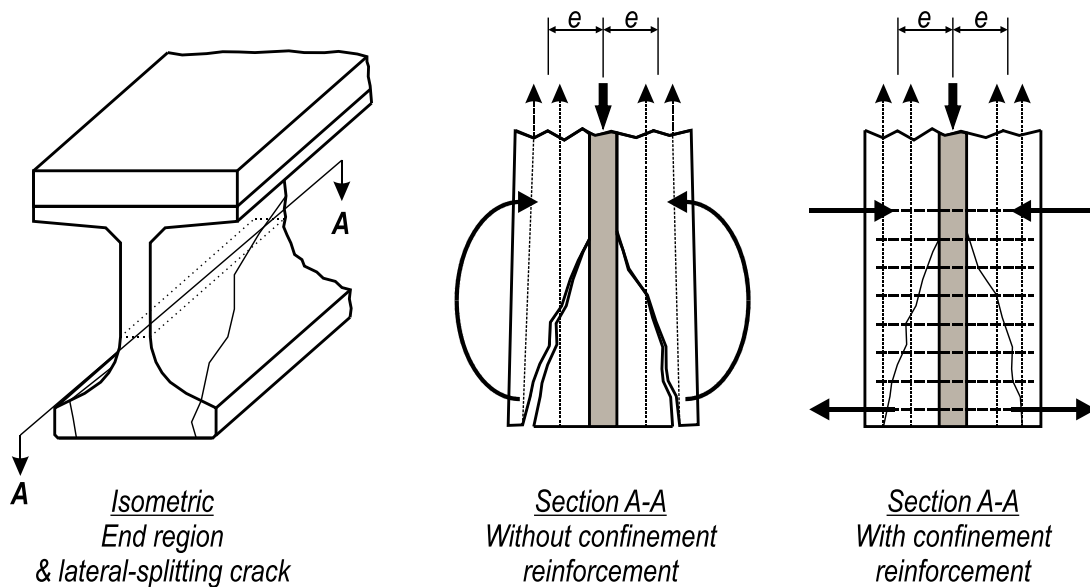

Fig. 5 Lateral-Splitting Failure

Isometric	*Section A-A*	*Section A-A*
End region	*Without confinement*	*With confinement*
& lateral-splitting crack	*reinforcement*	*reinforcement*

Fig. 6 Lateral-Splitting Failure Mechanics

LOAD TESTS HC AND VC

Specimens HC and VC had confinement reinforcement in the bottom flange and exhibited web-shear failure mode. Test results from these girders are presented and discussed together because of these similarities. The primary differences between HC and VC were the presence of horizontal reinforcement and the quantity of vertical reinforcement at the end of HC. Test results from these specimens are summarized in Fig. 8.

Cracks in HC and VC were first observed during the service load tests at 225 kip and 240 kip, respectively. Inclined web cracks between the load point and support were the first to be observed. These cracks partially closed during the unloading stages of the service load tests. The web crack in specimen HC had a maximum width of 0.004 in. at a shear of 244kip, and 0.002 in. after load was removed. In specimen VC the maximum crack width was 0.014 in. at a shear of 290kip, and 0.002 in. after load was removed.

Following the service load testing, specimens HC and VC were loaded to ultimate capacity. Stiffness in both specimens decreased gradually as load increased beyond the level of the service load tests. Since flexural cracks were not observed in either specimen, the loss in stiffness is attributed to formation and growth of diagonal cracks. Ultimate capacity was signaled by web crushing followed immediately by movement of the portion of the specimen above the inclined cracks relative to that below the inclined crack. This was the expected mode of failure and is typically classified as a web-shear failure. Loss of capacity after the web-shear failure was abrupt. Specimen HC supported a maximum shear of 766 kip and specimen VC supported a maximum shear of 698 kip.

Cracking entered the bottom flange during the latter stages of the ultimate load tests. These cracks are attributed in-part to the bottom flange mechanics demonstrated by Fig. 6. The bottom flange cracks, however, did not lead to lateral-splitting failure because specimens HC and VC had confinement reinforcement and bearing plates that were sufficient to carry transverse tensile forces at the member ends.

If the flexural capacity is low enough such that flexural cracks form near the support, then the strand transfer and development lengths are shortened, which can lead to flexural cracking and ultimately a bond-shear failure. LVDT data, however, indicate that strand slip during the tests was negligible. This was likely due to the relatively large quantity of strands, which resulted in a large prestress force and a small load demand per strand at ultimate capacity.
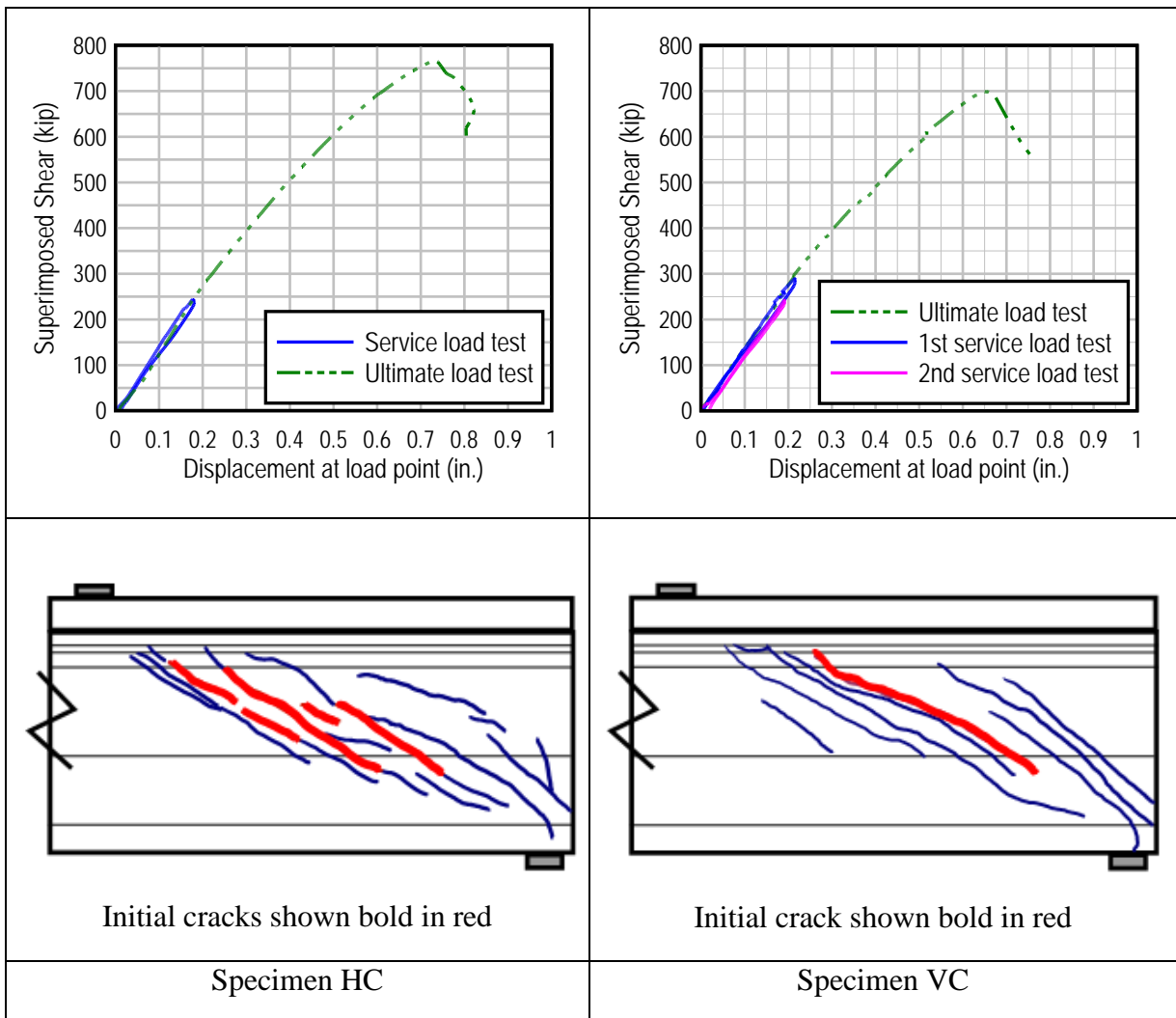
Fig. 7 – Summary of Results Specimens HC and VC

LOAD TESTS HU AND VU

Specimens HU and VU had no confinement reinforcement and exhibited similar behavior in load tests. As such, results from these specimens will presented and discussed together in this section. Test results are summarized in Fig. 9. The primary differences between specimens HU and VU were the presence of horizontal reinforcement and the quantity of vertical reinforcement in the end region of HU.

Cracks in HU and VU were first observed during the service load tests at 215 kip and 243 kip, respectively. The first cracks to be observed were web cracks inclined between the load point and support. The web crack in specimen HU had a maximum width of 0.004 in. at a shear of 230kip, and partially closed to 0.002 in. after load was removed. In specimen VU the maximum crack width was 0.001 in. at a shear of 243kip. Width of the web crack in VU did not change as load was removed after the service load test.

Following service load testing, specimens HU and VU were loaded to ultimate capacity. Stiffness in both specimens decreased gradually as load increased beyond the level of the service load tests. Loss in stiffness is attributed to formation and growth of diagonal cracks. Web cracks that formed at lower loads were observed to spread into the bottom flange during the latter stages of testing. Flexural cracks were not observed in either specimen.

The peak load corresponded to lateral-splitting failure in the bottom flange, which resulted in an abrupt loss of load. Specimen HU supported a maximum shear of 666 kip and specimen VU supported a maximum shear of 635 kip.

Strand slip was negligible in specimens HU and VU. As with specimens HC and VC, this observation is attributed to the relatively large quantity of fully bonded strands and to the lack of flexural cracks.
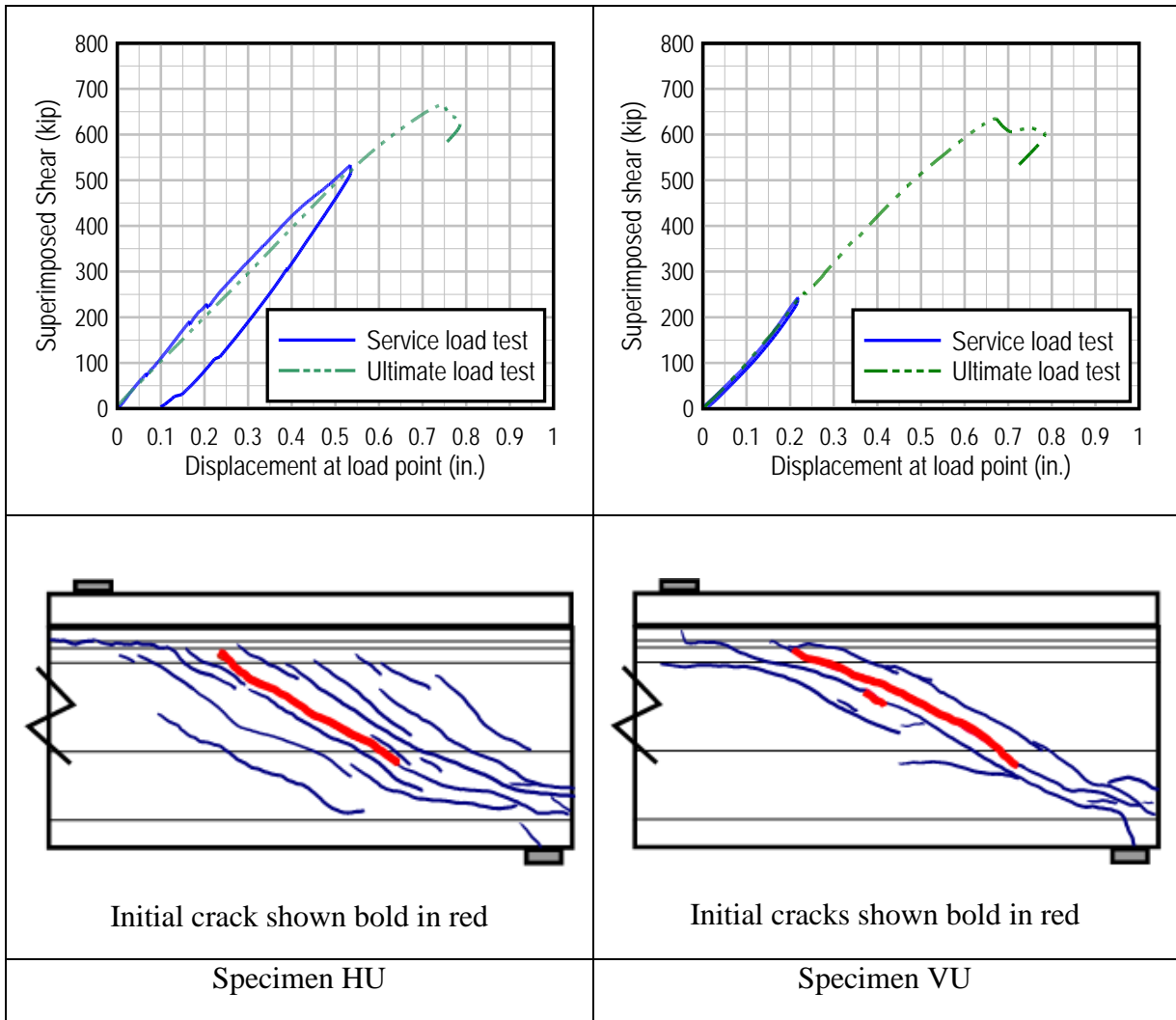
Fig. 8 – Summary of Results Specimens HU and VU

CONFINEMENT REINFORCEMENT AND BEARING PLATE FORCES

Specimens HC and VC had 16 separate confinement reinforcement assemblies distributed throughout the end region. Four assemblies in each specimen were instrumented with strain gages (Fig. 9). Instrumentation locations were selected to capture variations in confinement reinforcement behavior along the span length.

Data from strain gages were used to estimate transverse forces in the confinement reinforcement at ultimate load. Forces were calculated by multiplying experimental strain reported from the gages by the reinforcement cross-sectional area and steel elastic modulus. At locations where the confinement reinforcement was not instrumented with strain gages, the force was estimated using linear interpolation. Strain gages were also placed on the top and bottom of the steel bearing plates in all four specimens. Bearing plate forces were estimated by multiplying the average strain from the bearing plate gages by the plate cross-sectional area and elastic modulus.
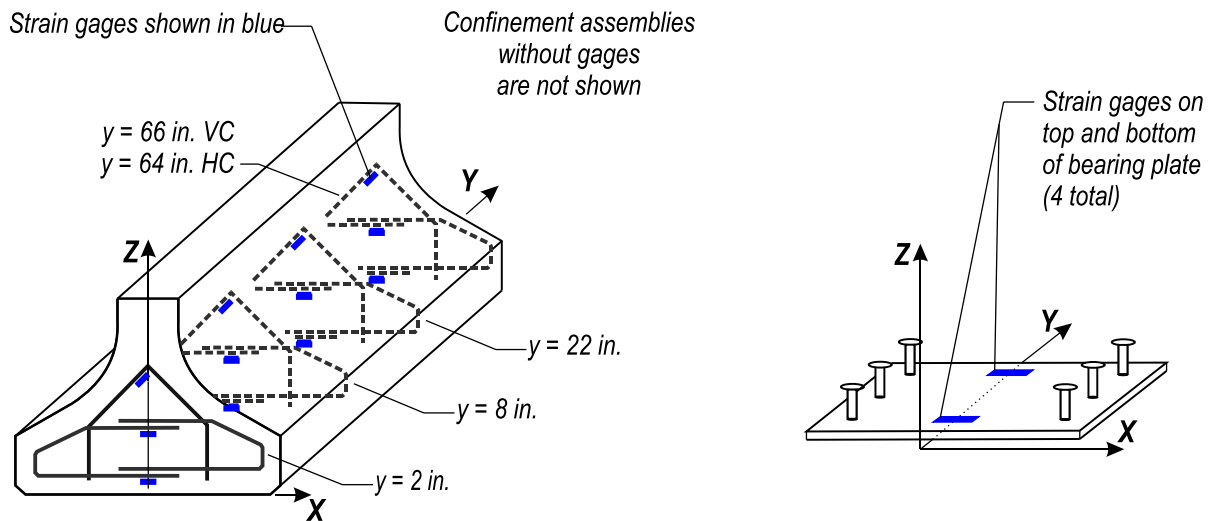
Fig. 9 Strain Gages on Confinement Reinforcement and Bearing Plates

Only strain due to applied load is included in the strain data presented in this paper. Self-weight and prestressing forces are also believed to affect behavior of confinement reinforcement and bearing plates.   Strain due to self-weight and prestressing forces are not considered. The effects of prestress force and self-weight are currently being studied by the authors and will be addressed in a forthcoming report for the FDOT[10].
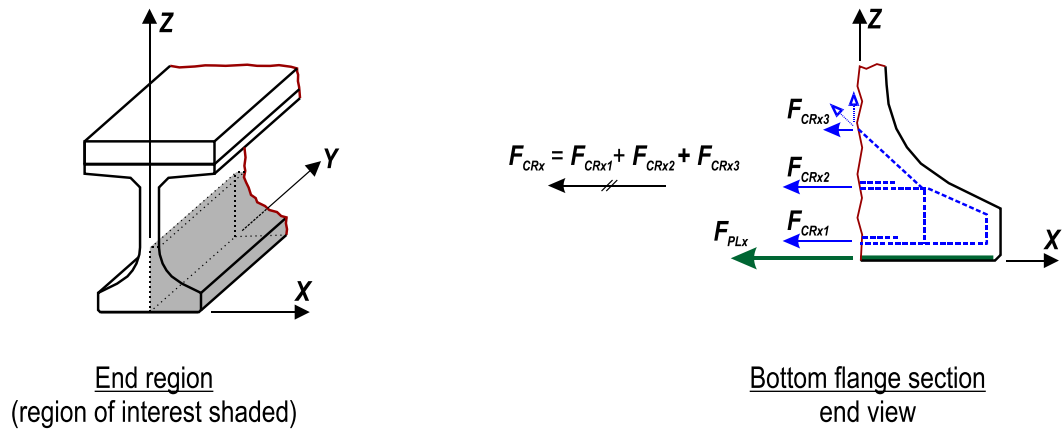
At ultimate load, stresses in the confinement reinforcement due to the applied load ranged from 20.6 ksi tension to 9.7 ksi compression.   Estimated forces in the confinement reinforcement and bearing plates are presented in Fig. 10 for specimens HC and VC. The estimated tensile force carried by all confinement reinforcement was 25.7 kip and 30.3 kip for specimens HC and VC, respectively. These forces equate to approximately 4% of the reaction at ultimate load. The largest confinement reinforcement forces occurred near the end of the specimens. At locations farther away from the end, the confinement reinforcement

carried compressive forces, thus, confirming the theoretical behavior presented in Fig. 6. This suggests that the optimum location for confinement reinforcement is as close the member end as possible.

The transition from tensile to compressive action in the confinement appears to have occurred at distances approximately 40in. and 50in. from the specimen ends (Fig. 10). The flexural depth (d) of the non-composite member was 49in. Comparing the distribution of confinement forces with the flexural depth shows that all tension in the confinement reinforcement occurred within d for the member end. Current AASHTO LRFD requirements specify that confinement reinforcement must extend at least $1.5d$ from the member end. The experimental results suggest that this requirement is conservative, and that more efficient placement of confinement reinforcement may be possible. Experimental results are also consistent with provisions from AASHTO Standard Specifications[12], which required that confinement reinforcement be placed over a distance d from the member end. Additional research is recommended to confirm the current result that d is a sufficient distance for placement of confinement reinforcement in FIB and similar girders. Other researchers[11] have also suggested that the required distribution of confinement reinforcement could be reduced to less than $1.5d$.

When specimens HC and VC were loaded to ultimate capacity the average transverse (x-x) tensile stress in the bearing plates due to the applied load was 11.6 ksi, which equates to a total force of approximately 69.9 kip. As noted earlier, confinement reinforcement in specimens HC and VC supported transverse tension forces of 25.7 kip and 30.3 kip, respectively. Thus the bearing plate carried on average 71% of the total transverse tension force and the confinement reinforcement carried the other 29%.

Tensile forces were also carried by the bearing plates in specimens without confinement reinforcement. The transverse tensile force at ultimate load in the bearing plate in specimen HU was 64.4 kip. The bearing plate force in specimen VU could not be calculated due to a strain gage malfunction. Although the data were incomplete to estimate the bearing plate force in VU, the remaining strain gages indicated tensile strains of a magnitude similar to the other specimens. For the three specimens where the bearing plate force could be calculated, the calculated force was approximately equal to 10% of the ultimate reaction force.

End region
(region of interest shaded)

$F_{CRx} = F_{CRx1} + F_{CRx2} + F_{CRx3}$

Bottom flange section
end view

Note: Forces shown below are due to applied load only.
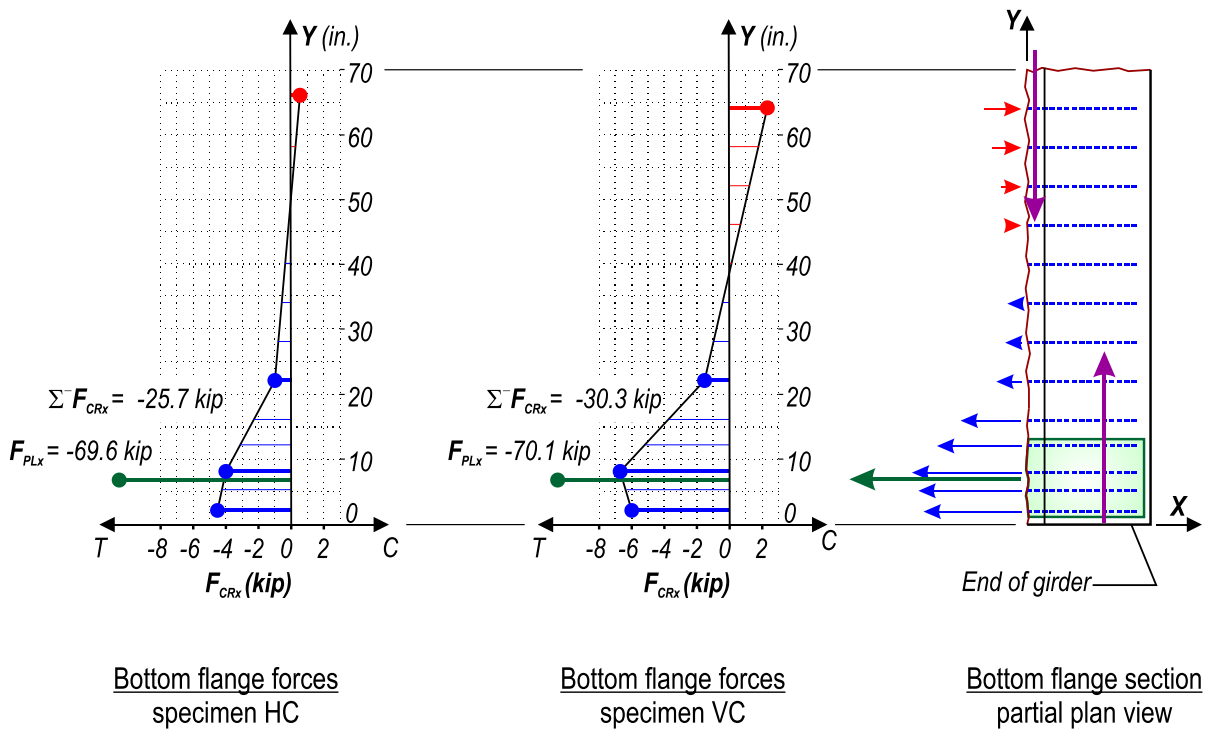The effects of prestress transfer are not included.

$\Sigma^- F_{CRx} = -25.7$ kip

$F_{PLx} = -69.6$ kip

$\Sigma^- F_{CRx} = -30.3$ kip

$F_{PLx} = -70.1$ kip

End of girder

Bottom flange forces
specimen HC

Bottom flange forces
specimen VC

Bottom flange section
partial plan view

Fig. 10 Distribution of Confinement Reinforcement and Bearing Plate Forces in Bottom
Flange at Ultimate Load

VARIABLE COMPARISON

Specimens with confinement reinforcement (HC and VC) had 12% more capacity on average than specimens without confinement reinforcement. Other research studies have reported similar increases in capacity due to confinement reinforcement[2,4,6]. Increased capacity in test specimens with confinement is attributed to the change in failure mode affected by the confinement reinforcement. By preventing lateral-splitting, confinement reinforcement improved the capacity of HC and VC, relative to specimens HU and VU.

Specimens HC and HU had additional horizontal and vertical reinforcement in the end region that was not present in specimens VC and VU. The additional reinforcement resulted in an increase in capacity of almost 10% in specimen HC relative to VC, and less than 5% increase in specimen HU relative to VU. The effectiveness of the additional reinforcement was greater between specimens HC and VC because the governing failure mode in these specimens was web-shear. Horizontal and vertical reinforcement in the web does not appear to have significant (less than 5%) effect on the lateral-splitting capacity.

The relationship between bearing plate force and reaction force at ultimate load was not affected by the presence of confinement reinforcement. Force in the bearing plate at ultimate load was equal to 10% of the reaction force in specimens with and without confinement reinforcement. Although the relationship between plate force and reaction force was independent of confinement reinforcement, the bearing plate alone was not sufficient to prevent lateral-splitting failure in specimens HU and VU. Thus bearing plates contributed to confinement of the bottom flange, but confinement reinforcement was also required to prevent lateral-splitting failure.

CODE COMPARISONS

Experimental capacity of each specimen is compared with code based nominal capacities in Fig. 11. Nominal capacities were calculated using the detailed method from ACI 318-11[13],the general procedure from AASHTO LRFD[8], and the longitudinal end region requirement from section 5.8.3.5 of AASHTO LRFD. Capacities from each method are referred to in Fig. 11 as ACI, AASHTO, and END REGION, respectively. All calculations used the tested material properties shown in Table 1.

The critical section for shear was located below the load point. Size and spacing of vertical reinforcement at the load point were the same for all specimens. The additional vertical reinforcement in specimens HC and HU was placed within 5ft of specimen ends and did not affect the nominal shear capacity calculations at the critical section. As such the ACI and AASHTO nominal capacities did not vary between specimens.

Specimens HC and HU contained more end region reinforcement than specimens VC and VU and hence had greater end region capacity. In calculating the end region capacities, an inclined crack was assumed to have formed between the inside edges of the bearing pad and load patch. This assumption is consistent with the inclination angle of cracks observed in the load tests.

The experimental capacity of each specimen exceeded the nominal shear capacity from ACI and AASHTO by at least 8%. Specimens HU and VU failed in a lateral-splitting mode and had lowest margins of safety. Code provisions used to calculate the nominal shear capacity do not consider lateral-splitting failure; lateral-splitting failure is not explicitly addressed anywhere in either ACI 318 or AASHTO LRFD. Although they do not consider lateral-splitting, nominal capacities from both codes were still conservative for specimens HU and VU.

For Florida I-Beam sections, the bottom flange geometry and detailing is consistent regardless of section depth. The FIB-54 used in the current study has the same bottom flange as the much deeper FIB-96. This is also the case for girders used in Washington and Nebraska; they have identical bottom flange details regardless of girder depth. Using consistent bottom flange details is beneficial for fabrication, but can also lead to undesirable outcomes in deep long-span girders if designs do not consider lateral-splitting failure. This is because nominal shear capacity increases with girder depth and lateral-splitting capacity does not. For deep girders, such as the FIB-96, is it possible that lateral-splitting is the critical failure mode and could occur at loads below the calculated nominal shear capacity. In such a case nominal shear capacity would be an unconservative measure of girder capacity. Work is underway by the authors to create a bottom flange design model that considers lateral-splitting.

From the current study it is known that the experimental lateral-splitting capacity of the FIB bottom flange with FDOT specified confinement reinforcement is at least 766 kip.

Multiplying 766 kip by a strength reduction factor of 0.85 results in a lateral-splitting capacity of 651 kip. Figure 12 compares the 651 kip capacity to the ultimate reaction force from various combinations of span length and girder spacing. Span and spacing combinations shown in the figure are at the extreme span and spacing limits for FIB-96 girders. Reaction forces were calculated using the FDOT LRFD Prestressed Beam[14] Mathcad design program, which is based on AASHTO LRFD loads and load combinations. Based on the comparisons shown in Figure 12, lateral-splitting failure is unlikely in girders detailed similar to HC. Lateral-splitting failure is of greater concern in girders with less-than-FDOT bottom flange confinement, such as specimen VU. Additional work is required to determine the effects of variables such as skew, bearing plates, and strand pattern on lateral-splitting capacity.

The end region capacities of all specimens were greater than the nominal shear capacities. Thus according to the AASHTO code, these specimens should have failed in shear prior to bond failure or yielding of strands and reinforcement in the end region. The AASHTO code result is consistent with test results from specimens HC and VC which failed in web-shear and gave no indication of strand bond failure or yielding.

The calculated end region capacities were less than the experimental capacity for all but specimen HU. This specimen did not have confinement reinforcement and failed in a lateral-splitting mode prior to reaching the calculated end region capacity. Had end region capacity controlled the design, the code calculated capacity would have been 10% larger than the experimental capacity (i.e., unconservative). As such, specimen HU provides another illustration of the need for a lateral-splitting design model.
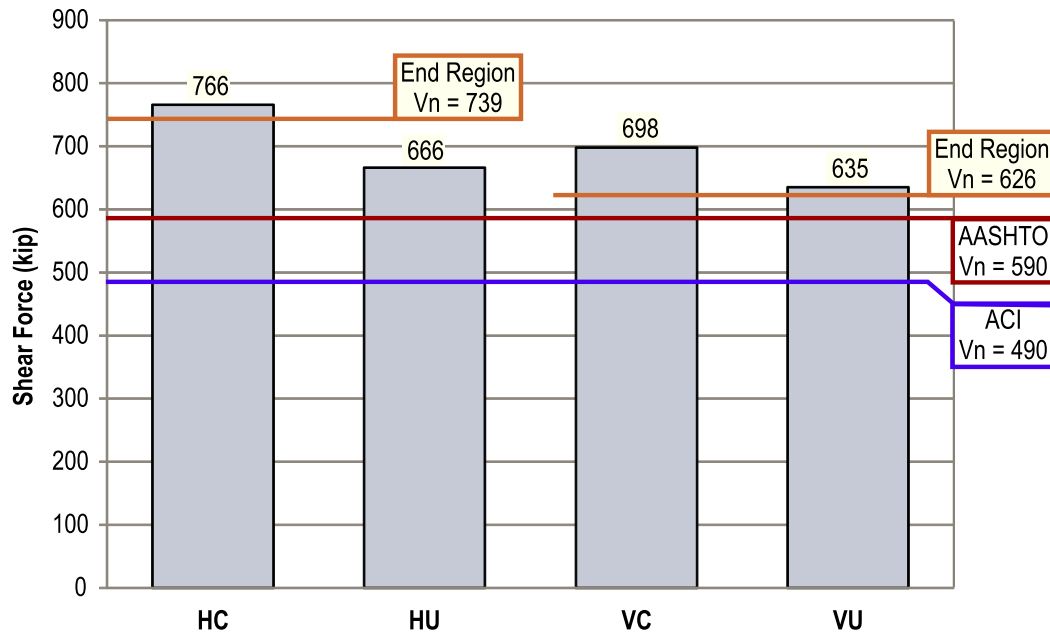

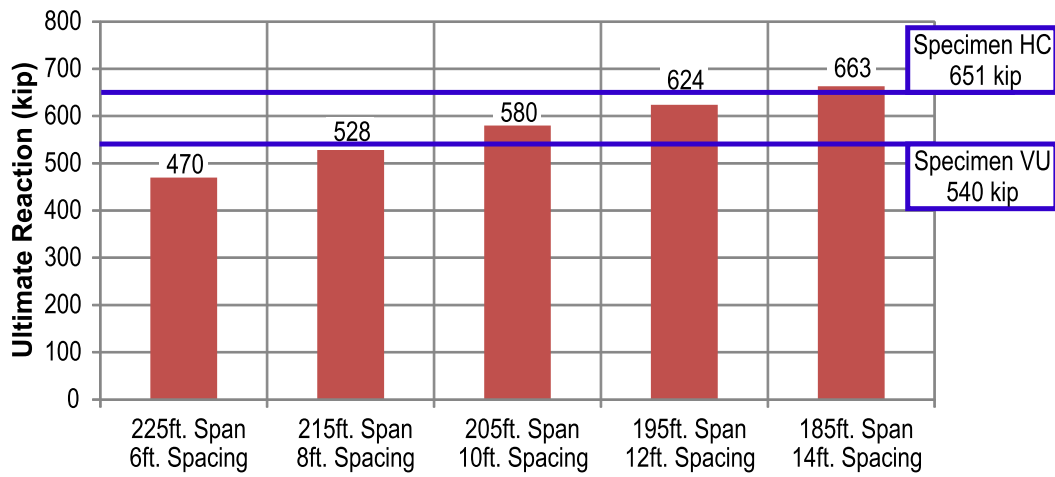Fig. 11 Experimental and Nominal Capacities

Fig. 12 Lateral-Splitting Capacity Compared with Ultimate Reaction Forces

SUMMARY AND CONCLUSIONS

Four load tests were conducted on FIB-54 pretensioned girders at a shear span-to-depth ratio of 1.8. Variables in the test program included the presence or lack of confinement reinforcement and the quantity of horizontal and vertical reinforcement in the end region. Each specimen had an embedded steel bearing plate. Forces in the confinement reinforcement and bearing plates at ultimate capacity were estimated using strain data. The following conclusions are made:

- Lateral-splitting failure was prevented in test specimens with confinement reinforcement. By preventing lateral-splitting, the confinement reinforcement improved capacity by an average of 12% over specimens without confinement reinforcement.
- The quantity of horizontal and vertical reinforcement in the end region of the specimens did not affect failure mode, but did affect ultimate capacity. The additional horizontal and vertical reinforcement increased capacity by an average of 7% relative to the capacity of specimens without the additional reinforcement.
- Transverse tensile stresses occur at the end of concrete girders due to applied loads and due to the eccentricity between prestressing forces in the outer flange and internal member forces. Transverse tensile stresses can lead to lateral-splitting failure if a sufficient load mechanism is not provided.
- Transverse tensile forces were carried by bearing plates and confinement reinforcement in the test specimens. Peak tension forces in the bearing plates and confinement reinforcement were equal to approximately 10% and 4% of the peak reaction, respectively.
- Embedded steel bearing plates carry transverse tension forces but are not sufficient to prevent lateral-splitting without confinement reinforcement.
- Strand slip was not observed in the test specimens. Absence of strand slip is attributed to the relatively high cracking moment due to the large number of strands in each specimen.
- Transverse tension forces in the bottom flange are greatest at the end of members directly above the bearing. In the test specimens all transverse tension forces were located within one member depth of the specimen end. Confinement reinforcement located over one member depth from the end was in compression. Thus, optimal placement of confinement reinforcement is as near to the end as practical and should extend at least one member depth from the end.
- There is need for a design model that addresses lateral-splitting failure in pretensioned I-girders.

ACKNOWLEDGEMENTS

REFERENCES

1. Russell, B., and Burns N., "Measured Transfer Lengths of 0.5 and 0.6 in. Strands in Pretensioned Concrete," *PCI Journal*. Sept.-Oct. 1996, pp. 44-54.
2. Csagoly, P. *A Shear Model for Prestressed Concrete Beams*. Florida Department of Transportation. Tallahassee, FL. 1991.
3. Llanos, G., Ross, B. and Hamilton, H. *Shear Performance of Existing Prestressed Concrete Bridge Girders*. Florida Department of Transportation. Tallahassee, FL. 2009.
4. Ross, B., Hamilton, H., Consolazio, G., "Experimental and Analytical Evaluations of Confinement Reinforcement in Pretensioned Concrete Beams," *Transportation Research Record.* No. 2251, 2011, pp. 59-67
5. Morcous, G., Hanna, K., Tadros, M. *Bottom Flange Reinforcement in NU I-Girders*. Nebraska Department of Roads. Lincoln, NE. 2010.
6. Shahway, M., Robinson, B., and B. de V. Batchelor. *An Investigation of Shear Strength of Prestressed Concrete AASHTO Type II Girders.* Florida Department of Transportation. Tallahassee, FL. 1993.
7. Aknoukh, A. *The Effect of Confinement on Transfer and Development Length of 0.7 Inch Prestressing Strands*. Concrete Bridge Conference. Phoenix, AZ. 2010.
8. AASHTO LRFD Bridge Design Specifications 4th Edition. American Association of State Highway and Transportation Officials. Washington, DC. 2007.
9. Florida Department of Transportation (FDOT). *Temporary Design Bulletin C09-03*. FDOT. Tallahassee, FL. 2009.
10. Ross, B. Hamilton, H., Consolazio G. *End Region Detailing of Pretensioned Concrete Bridge Girders*. Florida Department of Transportation. Tallahassee, FL. (In preparation)
11. Tadros, M., Badie, S., Tuan, C. *Evaluation and Repair Procedures for Precast/Prestressed Concrete Girders with Longitudinal Cracking in the Web*. National Cooperative Highway Research Program, Report 654. Transportation Research Board. Washington, DC. 2010.
12. AASHTO Standard Specifications for Highway Bridges 17th Edition. American Association of State Highway and Transportation Officials. Washington, DC. 2002.
13. ACI 318-11. Building Code Requirements for Structural Concrete. American Concrete Institute. Farmington Hills, MI. 2011.
14. Florida Department of Transportation (FDOT). *LRFD Prestressed Beam* version 3.2. Mathcad Program. Tallahassee, FL. 2010.